

# Synthesis, Characterization, Biological Properties, ADMET and Drug-likeness Analysis of Mn (II) complexes with Schiff Bases Derived from Sulphathiazole and 4-diethylaminosalicylaldehyde/Salicylaldehyde

Haruna, A.<sup>1</sup>, Sirajo, I.T.<sup>2</sup>, Rumah, M.M.<sup>3</sup> and Albashir, Y.<sup>4</sup>

<sup>1</sup>Department of Chemistry, Federal University Gusau, P.M.B 1001, Gusau, NIGERIA.

<sup>2</sup>Department of Pure and Industrial Chemistry, Bayero University, P.M.B 3011, Kano, NIGERIA.

<sup>3</sup>Department of Chemistry, Al-Qalam University Katsina, P.M.B 2137, Katsina, NIGERIA.

<sup>4</sup>Department of Chemistry, Federal University, Dutsinma, P.M.B 5001, Dutsinma, NIGERIA.

<sup>1</sup>Corresponding Author: [anasharunaabk@gmail.com](mailto:anasharunaabk@gmail.com)



<https://orcid.org/0000-0002-3455-8868>



[www.jrasb.com](http://www.jrasb.com) || Vol. 2 No. 6 (2023): December Issue

Received: 03-12-2023

Revised: 05-12-2023

Accepted: 07-12-2023

## ABSTRACT

Mn (II) complexes were synthesized with the Schiff base ligand obtained by the condensation of sulfathiazole with 4-diethylaminosalicylaldehyde/Salicylaldehyde. Their characterization was performed by elemental analysis, molar conductance, melting points, magnetic susceptibility, infrared, and UV-Vis spectral analysis. The results suggest that the Schiff bases and their complex are synthesized in excellent yield, molar conductance studies on the complexes indicated they were non-electrolytic. The IR data indicated that the Schiff base ligand is tridentate coordinated to the metallic ion with two N atoms from the azomethine group and thiazole ring and one O atom from the phenolic group. The electronic spectral study showed octahedral geometry for all the complexes which are further supported by magnetic moment values. The ligand and its complexes were screened against four bacterial and two fungal strains using the disk diffusion method. The antimicrobial evaluation results revealed that the metal (II) complexes exhibited higher antimicrobial activity than the free Schiff base ligand. The ADMET and drug-likeness studies of the synthesized ligands indicated that the Schiff base ligands fulfill Lipinski's, Ghose, Veber, Egan, and Mugges rules but the complexes showed some deviations. They also displayed low toxicity levels.

**Keywords-** Schiff base; complexes; antimicrobial activity, drug-likeness.

## I. INTRODUCTION

Schiff bases continue to be important in coordination chemistry and draw interest from scientists because of their intriguing physical and chemical characteristics. Hugo Schiff reported the first synthesis of a Schiff base, which results from the reaction of an aldehyde or ketone with a primary amine [1][2]. The preparation of metal complexes formed from Schiff bases involves adding the Schiff-base ligand to a metal

precursor in the proper ratio under the right experimental conditions [3].

Schiff bases and their metal complexes have been employed by researchers as chelating ligands in coordination chemistry as catalysts [4][5][6], as corrosion inhibitors [7][8], as a dye [9]. Biologically, they have been tested as antibacterial [5][10][11], antifungal [12][13], antitumor [14], anticancer [15] antioxidant [16][17], antiviral [18] and anti-inflammatory [19] among others. Therefore, the rapid development of novel chemotherapeutic Schiff base

ligands and their metal complexes is essential for bio-inorganic and medicinal chemistry [20].

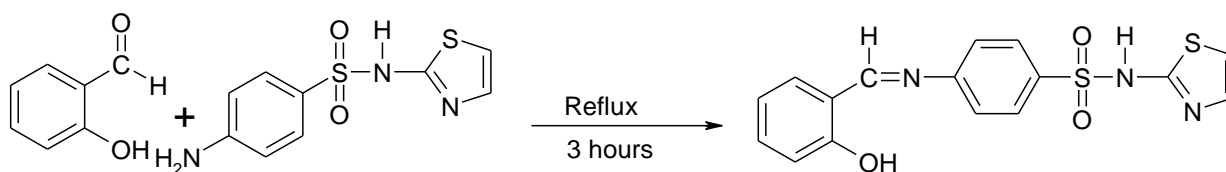
New Co(II), Ni(II), and Cu(II) complexes containing the Schiff base ligand were synthesized, according to Reiss *et al.*, [21], by condensation of sulfathiazole with salicylaldehyde. Elemental analysis, molar conductance, spectroscopic methods (IR, diffuse reflectance, UV-Vis-NIR), magnetic moments, thermal analysis, and calorimetry (thermogravimetry/derivative thermogravimetry/differential scanning calorimetry) were used to characterize them, and powder X-ray diffraction results were used to explain their morphology and crystal systems. The Schiff base and its metal complexes were tested against some bacterial strains (*Escherichia coli*, *Pseudomonas aeruginosa*, *Staphylococcus aureus*, and *Bacillus subtilis*). The results indicated that the antibacterial activities of all metal complexes were better than that of the Schiff base.

Our research work was aimed at the synthesis and characterization of the Mn (II) complexes with Schiff bases derived from Sulphathiazole and 4-diethylaminosalicylaldehyde/Salicylaldehyde. The work was extended to study the ADMET and drug-likeness, as well as the biological properties of the ligand and its metal complexes synthesized by evaluating their biological activity on different assay systems.

## II. METHODOLOGY

### 2.1 Materials

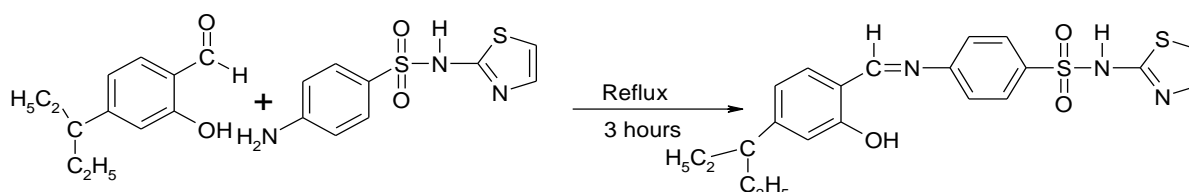
The chemicals and reagents that were used for this study are sulphathiazole, 4-diethylaminosalicylaldehyde, salicylaldehyde, ethanol, N,N-dimethylformamide, methanol, manganese (II) chloride, dimethyl sulfoxide (DMSO), were of analytical grade and used without further purification.



Scheme 1: 4-(2-hydroxybenzylidene)amino]-N-thiazole-2-ylbenzenesulphonamide

### 2.4 Synthesis of 4[(4,6-Dimethylamino-2-hydroxy-benzylidene)amino]-N-thiazole-2-ylbenzenesulphonamide

2.55 g sulphathiazole dissolved in 25 ml ethanol was mixed with 25 ml ethanolic solution of 4-



Scheme 2: 4[(4,6-Dimethylamino-2-hydroxy-benzylidene)amino]-N-thiazole-2-ylbenzenesulphonamide

### 2.2 Instrumentation

Elemental (C, H, and N) analysis data were obtained by using Series II CHNS/O 2400 Perkin Elmer elemental analyzer. Metal contents were determined experimentally by AAS. Mass spectra were recorded using a SHIMADZU GC-MS. Infrared spectral analysis was determined using Fourier transform infrared spectrophotometer (FTIR-8400S) range 4000-400 $\text{cm}^{-1}$ . Electrical conductance was measured using Jenway conductivity meter model 4010 range 20-200 $\mu\text{s}$  at room temperature in DMSO solution. Decomposition/ melting temperature were recorded using Stuart melting point apparatus SMP 10. Magnetic susceptibility was determined using magnetic susceptibility balance MKI Sherwood scientific ltd The magnetic susceptibility of the metal complexes were calculated using the relation  $\mu_{\text{eff}} = 2.828(\chi_{\text{m}} \cdot T)^{1/2}$  BM where  $\chi_{\text{m}}$  is the molar susceptibility corrected using Pascal's constants for diamagnetism of all atoms in the compounds. Weighing was conducted using electrical Melter balance model AB54. The electronic spectra of the synthesized compounds were recorded on a Perkin-Elmer spectrophotometer lambda 35 in the 200-700 nm range. A free web tool (SwissADME) was used for ADMET and drug-likeness analysis.

### 2.3. Synthesis of 4-(2-hydroxybenzylidene)amino]-N-thiazole-2-ylbenzenesulphonamide

The 4-(2-hydroxybenzylidene)amino]-N-thiazole-2-ylbenzenesulphonamide was prepared according to Scheme 1. An equimolar mixture of sulphathiazole dissolved in 25 mL of ethanol and salicylaldehyde in 25 mL of ethanol was refluxed for 3 h with a catalytic amount of glacial acetic acid. The mixture was kept for evaporation at room temperature. The yellow-orange colored solid obtained was washed with ethanol, and dried..

diethylaminosalicylaldehyde (1.93 g, 0.01 mol). The resulting solution was refluxed for 4 hours and then cools to room temperature. On cooling, precipitate formed which was filtered, washed with ethanol, recrystallized and then dried in dessicators over anhydrous  $\text{CaCl}_2$  [22].

### 2.5 Synthesis of the Metal Complexes

The complexes were prepared according to literature reported by Chauhan *et al.*, [23], by mixing hot ethanolic solutions (3.55 g, 0.01 mol) 25 ml of N-(4,6-Dimethylpyrimidin-2-yl)-4-[(2-hydroxylydene)amino]benzenesulphonamide and (4.53 g, 0.01 mol) 25 ml of 4[(4-Diethylamino-2-hydroxy-benzylidene)amino]-N-(4,6-dimethylpyrimidin-2-yl)benzenesulphonamide with a hot ethanolic solution of (0.005 mol) 25ml of manganese (II) chloride. The resulting mixtures were refluxed for 8hrs, the complex obtained in each case was cool to room temperature, filtered, and washed with ethanol and diethyl-ether several times to remove any excess ligand. Finally, the complex was dried over anhydrous CaCl<sub>2</sub> in desiccators.

**Ligand (L<sup>1</sup>):** Yield 90%; mp. 186°C; Color Yellow Orange; Molecular formula C<sub>16</sub>H<sub>13</sub>S<sub>2</sub>N<sub>3</sub>O<sub>3</sub>; Elemental analyses: (Cal) C, 53.47 %; H, 3.64 %; N, 11.69 %; Found: C, 53.91 %; H, 3.87 %; N, 12.40%; GC-MS [M+H]<sup>+</sup> m/z 355.2 FTIR (KBr (cm<sup>-1</sup>)): 3115 ν(O-H), 1618 ν(HC=N)azm, ν(HC=N) thiazole ring 1348/1138 ν(SO<sub>2</sub>)(Asym)/ν(SO<sub>2</sub>)(Sym) (UV/Vis λ<sub>max</sub> cm<sup>-1</sup>): 249 (π → π\*), and 269 ((n → π\*)).

**Ligand (L<sup>2</sup>):** Yield 82%; mp. 180°C; Color Yellow; Molecular formula C<sub>20</sub>H<sub>22</sub>S<sub>2</sub>N<sub>4</sub>O<sub>3</sub>; Elemental analyses: (Cal) C, 55.79 %; H, 5.15 %; N, 13.01 %; Found: C, 56.12 %; H, 5.26 %; N, 14.00%; GC-MS [M+H]<sup>+</sup> m/z 429.2 FTIR (KBr (cm<sup>-1</sup>)): 3134 ν(O-H), 1628 ν(HC=N) azm, ν(HC=N) thiazole ring, 1354/1138 ν(SO<sub>2</sub>)(Asym)/ν(SO<sub>2</sub>)(Sym) (UV/Vis λ<sub>max</sub> cm<sup>-1</sup>): 204 (π → π\*), and 228 ((n → π\*)).

**[Mn (L<sup>1</sup>)<sub>2</sub>].2H<sub>2</sub>O:** Yield 74 %; decomp temp. 263°C; C<sub>32</sub>H<sub>28</sub>S<sub>4</sub>MnN<sub>8</sub>O<sub>8</sub>; Elemental analyses: (Cal) C, 47.58 %; H, 3.48 %; Mn, 6.80 %; N, 10.40 % Found: C, 48.06 %; H, 3.87 Mn, 7.20 %; N, 10.35 %; Molar conductance (Ω cm<sup>2</sup> mol<sup>-1</sup>): 9.53; μ<sub>eff</sub>(B. M): 5.7; FTIR (KBr (cm<sup>-1</sup>)): 3450 ν(O-H), 1611 ν(HC=N) azm, ν(HC=N) thiazole ring, 1343/1149 ν(SO<sub>2</sub>)(Asym)/ν(SO<sub>2</sub>)(Sym), 569 ν(Mn-O), 456 ν(Mn-N). (UV/Vis λ<sub>max</sub> cm<sup>-1</sup>): 255 (π → π\*), 270 ((n → π\*), 370 (C.T), 437 (6<sub>A<sub>1g</sub></sub> → 4<sub>T<sub>1g</sub></sub>).

**[Mn (L<sup>2</sup>)<sub>2</sub>].2H<sub>2</sub>O:** Yield 75 %; decomp temp. 269°C; Color orange; Molecular formula C<sub>40</sub>H<sub>46</sub>S<sub>4</sub>MnN<sub>8</sub>O<sub>8</sub>; Elemental analyses: (Cal) C, 50.57 %; H, 4.65 %; Mn, 5.58 %; N, 11.80 % Found: C, 51.05 %; H, 4.97 Mn, 5.69 %; N, 12.18 %; Molar conductance (Ω cm<sup>2</sup> mol<sup>-1</sup>): 9.32; μ<sub>eff</sub>(B. M): 5.9; FTIR (KBr (cm<sup>-1</sup>)): 3443 ν(O-H), 1607 ν(HC=N) azm, ν(HC=N) thiazole ring 1350/1138 ν(SO<sub>2</sub>)(Asym)/ν(SO<sub>2</sub>)(Sym), 526 ν(Mn-O), 452 ν(Mn-N). (UV/Vis λ<sub>max</sub> cm<sup>-1</sup>): 208 (π → π\*), 223 ((n → π\*), 381 (C.T), 400 (6<sub>A<sub>1g</sub></sub> → 4<sub>T<sub>1g</sub></sub>).

### 2.5 Antibacterial Activity

Two Gram-positive bacteria (*Bacillus subtilis* and *Staphylococcus aureus*) and two Gram-negative bacteria (*Escherichia coli* and *Klebsiella pneumoniae*) were employed to test the antibacterial activity of the free ligands and the Mn (II) complexes using the paper disk diffusion technique. The medium was prepared using Mueller-Hinton agar. Dimethyl sulfoxide and

ciprofloxacin were employed as positive and negative controls, respectively. The bacterial strains were tested with 0.05, 0.1, 0.15, and 0.2 mg/mL concentrations. In the process, each of the compounds dissolved in DMSO at concentrations of 0.05, 0.1, 0.15, and 0.2 mg/mL, and 6 mm diameter Whatman filter paper disks were soaked in a 1 mL solution of the above two concentrations. Then, these saturated paper disks were inoculated at the center of a Petri dish having a bacterial lawn. The plates were incubated at 37 °C for 48 h, and then the inhibition zone was determined by measuring the diameter of the inhibition zone [24][25][26].

### 2.6 Antifungal Activity

Disk diffusion method was also used for antifungal susceptibility of synthesized compounds with same concentrations in DMSO as mentioned above but *Aspergillus niger* and *Candida albicans* were used as the fungal strain and fluconazole as reference drug. Petri plates were prepared by pouring 30 mL of potato dextrose agar (PDA) medium. The test organisms were inoculated on a solidified agar plate with the help of a micropipette and spread and allowed to dry for 10 min. A sterile cotton swab was dipped into a standardized microbes test suspension and used to evenly inoculate the entire surface of the PDA plates. Using sterile forceps, the sterile filter papers (6 mm diameter) containing discs were loaded with given concentrations of each sample, control, and the standard solution were laid down on the surface of an inoculated agar plate. The plates were incubated at 37 °C for 48 h. After the completion of incubation period, the diameters of the inhibition zones generated by each test compound against fungal growth were measured using antibiogram zone measuring scale [27][28].

### 2.7 Drug-Likeness and ADMET Prediction

The two-dimensional (2D) structures were transformed into a simplified molecular input line entry system (SMILES) using the free web program SwissADME in order to estimate the in silico pharmacokinetics parameters and other molecular features. Related researches have employed this strategy with success. SwissADME also predicted physicochemical qualities, lipophilicity, skin permeability, drug-likeness for Lipinski's rule of five, and pharmacokinetics parameters (Diana *et al.*, 2017; Dong *et al.*, 2018). Using ADMETLAB 2.0, the ligands' and their complex's organ toxicities, toxicological endpoints, and LD50 were predicted. The analyses of the compounds were compared with those of fluconazole, sulphathiazole, and ciprofloxacin [28][29]

## III. RESULTS AND DISCUSSION

### 3.1 Chemistry

The synthesized Schiff bases (4-(2-hydroxybenzylidene)amino)-N-thiazole-2-ylbenzenesulphonamide and 4[(4,6-Dimethylamino-2-hydroxy-benzylidene)amino]-N-thiazole-2-

ylbenzenesulphonamide) are highly stable at room temperature and nonhygroscopic and found to be soluble in methanol, ethanol, DMF and DMSO, whereas their complexes are soluble only in DMF and DMSO, but are insoluble in water. Metal complexes were obtained from the reaction of the ligands with manganese (II) chlorides. These solid complexes are colored, and stable in air at room temperature, and are readily soluble in DMSO and DMF but slightly soluble in ethanol and methanol but are insoluble in water. The melting points of the complexes were higher than that of the Schiff base ligand indicating that the complexes are more stable than the ligand. Obtained values in the elemental analysis are in good agreement with those calculated. The percentages of metals in the complexes were determined experimentally

(using AAS) to be in good agreement with the calculated values. Elemental analysis and analytical data agree well with the proposed formulation of the Schiff base ligands and their Mn (II) complex. These data suggested a 1:2 metal-to-ligand ratio of the complexes. These results are presented in table 1.

### 3.2 Conductivity Measurements

At room temperature, the molar conductance values of the produced compounds in  $10^{-3}$  M DMSO were determined. The produced compounds' conductance values were less than  $10 \text{ Ohm}^{-1}\text{cm}^2\text{mol}^{-1}$ , indicating that they were non-electrolytic in nature. This implied that no anions were present outside of the complexes' coordination sphere [18][30].

**Table 1: Physical and analytical data of the Schiff base ligands and their Mn (II) complex**

| Compounds  | colour           | M.p. (°C) | Yield % | $\Lambda_m(\text{Ohm}^{-1}\text{cm}^2\text{mol}^{-1})$ | $\mu_{\text{eff}}$ (BM) | Elemental analyses, calc (Found)% |                |                  |              |
|--|------------------|-----------|---------|--|-------------------------|-----------------------------------|----------------|------------------|--------------|
|  |                  |           |         |  |                         | C                                 | H              | N                | Mn           |
| L <sup>1</sup>   | Yellow           | 186       | 90      | -  | -                       | 53.47<br>(53.91)                  | 3.64<br>(3.87) | 11.69<br>(12.40) | -            |
| L <sup>2</sup>   | Yellow<br>Orange | 180       | 82      | -  | -                       | 55.79<br>(56.12)                  | 5.15<br>(5.26) | 13.01<br>(14.00) | -            |
| [Mn (L <sup>1</sup> ) <sub>2</sub> ].2H <sub>2</sub> O | Brown            | 263       | 74      | 9.53   | 5.7                     | 47.58<br>(48.06)                  | 3.48<br>(3.87) | 10.40<br>(10.35) | 6.80<br>7.20 |
| [Mn (L <sup>2</sup> ) <sub>2</sub> ].2H <sub>2</sub> O | Orange           | 269       | 75      | 9.32   | 5.9                     | 50.57<br>(51.05)                  | 4.65<br>(4.97) | 11.80<br>(12.18) | 5.58<br>5.69 |

### 3.3 Electronic Spectral and Magnetic Moments

The UV-Vis spectra of the ligands and their Mn (II) complex are explained in Table 2. In the spectrum of L<sup>1</sup>, peak appeared at 249 nm and is attributed to the  $\pi \rightarrow \pi^*$  transition; peak at 269 nm was attributed to the  $n \rightarrow \pi^*$  transitions. The electronic data of the Mn(II) complex with L<sup>1</sup> shows bands at 255, 270, 378 and 437 nm. Peaks at 255 and 270 nm are assignable to intraligand transition. Peak at 378 nm was attributed to charge transfer. The magnetic moment value is 5.7 B.M and presented in Table 1. The band at 437 nm is as a result of d-d transition for  $6_{A_{1g}} \rightarrow 4_{T_{1g}}$  (F) which indicates the presence of Mn(II) complex in octahedral structure [32]. In the case of L<sup>2</sup>, peak appeared at 204 nm which is attributed to the  $\pi \rightarrow \pi^*$  transition, peak at 228 nm was attributed to the  $n \rightarrow \pi^*$  transitions. The electronic data

of the Mn(II) complex show bands at 208 and 228 nm assignable to intraligand transition. Peak at 381 nm is attributed to charge transfer. Peaks at 400 was attributed to d-d transitions of the type  $6_{A_{1g}} \rightarrow 4_{T_{1g}}$  (F). The magnetic moment value is 5.9 B.M (Table 1) which indicates the presence of Mn(II) complex in octahedral structure (Nazeer, 2021; [32][32].

### 3.4 Mass Spectra

The mass spectrum of the 4-(2-hydroxybenzylidene)amino]-N-thiazole-2-ylbenzenesulphonamide and 4[(4,6-Dimethylamino-2-hydroxy-benzylidene)amino]-N-thiazole-2-ylbenzenesulphonamide showed a molecular ion peak at  $m/z$  [M+H]<sup>+</sup> 355.2 and 429.2  $m/z$  [M+H]<sup>+</sup> respectively which is consistent with their respective molecular weights.

**Table 2: Electronic Spectra of the Ligands and their Mn(II) complex**

| Compounds  | Absorption         | Transition   |
|--|--------------------|--|
| L <sup>1</sup>   | 249, 269           | $\pi \rightarrow \pi^*$ , $n \rightarrow \pi^*$  |
| L <sup>2</sup>   | 204, 228           | $\pi \rightarrow \pi^*$ , $n \rightarrow \pi^*$  |
| [Mn (L <sup>1</sup> ) <sub>2</sub> ].2H <sub>2</sub> O | 255, 270, 370, 437 | $\pi \rightarrow \pi^*$ , $n \rightarrow \pi^*$ C.T, $6_{A_{1g}} \rightarrow 4_{T_{1g}}$ |
| [Mn(L <sup>2</sup> ) <sub>2</sub> ].2H <sub>2</sub> O  | 208, 223, 381, 400 | $\pi \rightarrow \pi^*$ , $n \rightarrow \pi^*$ C.T, $6_{A_{1g}} \rightarrow 4_{T_{1g}}$ |

### 3.5 FT-IR Spectral Analysis.

The binding mode of the Schiff base ligands to the metal ions in complexes was determined by comparing the FT-IR spectrum of the sulphathiazole and free ligand with the spectra of the metal (II) complexes. The bands of 3350 and 3320  $\text{cm}^{-1}$  assigned to the  $\nu(\text{NH}_2)$  asymmetric and symmetric stretching vibrations in the sulphathiazole spectrum disappeared from the ligands' spectra, indicating that the amine group has, as expected, been transformed into an azomethine peak. The salicylaldehyde carbonyl's absence provided as supporting information for this.

The newly formed band at 1618  $\text{cm}^{-1}$  for  $\text{L}^1$  and 1611  $\text{cm}^{-1}$  for  $\text{L}^2$ , which is attributable to the  $\nu(\text{C}=\text{N})$  azomethine group, also supported the formation of the anticipated Schiff base ligand [31]. The Mn (II) complexes with  $\text{L}^1$  and  $\text{L}^2$  were found to have C=N

stretching frequencies at 1611  $\text{cm}^{-1}$  and 1607  $\text{cm}^{-1}$ , respectively. The shifting of the ligands' azomethine peaks showed that the Schiff base was being coordinated through the azomethine nitrogen [33]. In the sulfathiazole and Schiff base spectra, the (C=N) thiazole ring stretching vibration appeared at 1540  $\text{cm}^{-1}$ ; however, it was shifted to lower frequencies at 1480–1485  $\text{cm}^{-1}$  in the IR of the complexes, indicating that the Schiff base was coordinated with the central metallic ion through the N thiazole atom [32]. The spectra of the metal complexes revealed a few new bands in the 507-574  $\text{cm}^{-1}$  and 457-470  $\text{cm}^{-1}$  ranges that were attributed to  $\nu(\text{M}-\text{N})$  and (M-O) stretching vibrations [15]. It should be observed that these peaks were absent from the spectra of the Schiff base, indicating that the metal ion was coordinated by the Schiff base ligand molecule's phenolic oxygen and azomethine nitrogen [32].

**Table 3: Assignments of the IR spectra (frequency:  $\nu \text{ cm}^{-1}$ ) of sulfathiazole,  $\text{L}^1$  and  $\text{L}^2$ , and their Mn (II) complex**

| STZ  | $\text{L}^1$ | $\text{L}^2$ | $[\text{Mn}(\text{L}^1)_2] \cdot 2\text{H}_2\text{O}$ | $[\text{Mn}(\text{L}^2)_2] \cdot 2\text{H}_2\text{O}$ | Assignments                         |
|------|--------------|--------------|---|---|-------------------------------------|
| 3350 | -            | -            | -   | -   | $\nu(\text{NH}_2)$ Sysm             |
| 3320 | -            | -            | -   | -   | $\nu(\text{NH}_2)$ Asysm            |
| -    | -            | -            | 3200  | 3443  | $\nu(\text{H}_2\text{O})$           |
| -    | 3115         | 3134         | -   | -   | $\nu(\text{OH})$ phenolic           |
| -    | 1618         | 1628         | 1622  | 1607  | $\nu(\text{C}=\text{N})$ azomethine |
| 1540 | 1540         | 1540         | 1480  | 1485  | $\nu(\text{C}=\text{N})$ thiazole   |
| 1348 | 1346         | 1354         | 1346  | 1350  | $\nu(\text{SO}_2)$ Asym             |
| 1138 | 1141         | 1138         | 1149  | 1138  | $\nu(\text{SO}_2)$ Sym              |
| -    | -            | -            | 533   | 855   | $\nu(\text{M}-\text{O})$            |
| -    | -            | -            | 533   | 526   | $\nu(\text{M}-\text{N})$            |

### 3.6 Antimicrobial Activity

The synthesized compounds were evaluated (in vitro) for their microbial activities against four pathogenic bacteria and two fungal strains. The results are presented in Table 3. The inhibition zone values of the studied complexes showed their potential antimicrobial activity when compared to a standard drug. The complexes showed pronounced activity against gram-positive bacteria and considerable activity against the gram-negative bacteria than the free ligands. All the complexes showed moderate activity against fungal strain. These results are in line with previous reports [34]. The increasing antimicrobial activity of the metal chelates with the increase in concentration is due to the effect of metal ions on the normal cell process. Such increased activity of the metal chelates can be explained based on chelation theory. Lipid is an important factor that controls antimicrobial activity. Tweedy's chelation theory, explains that the ion polarity of the complex is reduced by overlapping of the ligand orbitals and the exchange of the partial positive charge of the metal ion

to the donor atoms of the ligand; thereby, the delocalization of p-electrons increases on the chelate ring and improves the lipophilicity of the complexes. The increment in lipophilicity increases the penetration of the complex into the lipid's membrane and blocks the metal binding sites in the microorganisms' enzymes, disturbing the process of cell respiration and the synthesis of proteins, thereby inhibiting the growth of the organism. Furthermore, the mode of action of the compounds may involve the formation of hydrogen bond through azomethine group with the active centers of cell constituents, resulting in interference with the normal cell process[8].

It is evident from the data that the complexes were more toxic towards Gram (+) strains as compared to Gram (-) strains which may be attributed to the fact that the cell walls of Gram (-) strains have more antigenic properties due to the presence of an outer lipid membrane of lipopolysaccharides. It also found to be more active against the bacterial strains than in the fungal strains.

**Table 5: Antimicrobial screening data for the Schiff base ligand and its metal (II) complexes at concentrations of 50, 100, 150, and 200 µg/mL.**

| Sample   | Zone of inhibition in mm* against bacterial/Fungal strains |               |           |               |              |                |             |  |
|--|--|---------------|-----------|---------------|--------------|----------------|-------------|--|
|  | Conc.  | Gram Positive |           | Gram Negative |              | Fungal Strains |             |  |
|  |  | B. subtilis   | S. aureus | E. coli       | K. pneumonia | A. niger       | C. albicans |  |
|  |  | (µg/mL)       |           |               |              |                |             |  |
| L <sup>1</sup>   | 50   | 12            | 11        | 10            | 10           | 10             | 10          |  |
|  | 100  | 15            | 14        | 13            | 14           | 13             | 14          |  |
|  | 150  | 18            | 17        | 15            | 16           | 16             | 16          |  |
|  | 200  | 20            | 19        | 18            | 19           | 18             | 19          |  |
| L <sup>2</sup>   | 50   | 12            | 12        | 10            | 11           | 10             | 11          |  |
|  | 100  | 14            | 14        | 13            | 14           | 12             | 13          |  |
|  | 150  | 18            | 17        | 15            | 17           | 15             | 15          |  |
|  | 200  | 21            | 20        | 18            | 19           | 18             | 19          |  |
| [Mn (L <sup>1</sup> ) <sub>2</sub> ].2H <sub>2</sub> O | 50   | 14            | 13        | 13            | 13           | 12             | 12          |  |
|  | 100  | 16            | 16        | 15            | 16           | 14             | 15          |  |
|  | 150  | 20            | 18        | 18            | 18           | 17             | 18          |  |
|  | 200  | 23            | 22        | 20            | 21           | 19             | 20          |  |
| [Mn (L <sup>2</sup> ) <sub>2</sub> ].2H <sub>2</sub> O | 50   | 14            | 13        | 12            | 13           | 12             | 13          |  |
|  | 100  | 18            | 16        | 14            | 16           | 15             | 16          |  |
|  | 150  | 21            | 19        | 17            | 19           | 17             | 18          |  |
|  | 200  | 24            | 22        | 20            | 22           | 19             | 21          |  |
| SMT  | 150  | 15            | 14        | 13            | 14           | 13             | 13          |  |
| Ciprofloxacin  | 150  | 22            | 21        | 18            | 20           | -              | -           |  |
| Fluconazole  | 150  | -             | -         | -             | -            | 26.7           | 27.3        |  |
| DMSO   | -  | -             | -         | -             | -            | -              | -           |  |

### 3.7 Drug-Likeness and ADMET Predictions

Because of their problematic toxicity issues and subpar pharmacokinetics, many drugs fail during the drug development process. Issues that arise during drug development could be resolved early on. In silico ADMET techniques are utilized to assess this problem. These ADMET factors reveal how chemical substances behave inside living organisms.

#### 3.7.1 Physicochemical Parameters Generated Using SwissADME Tool

The ligands and their metal complexes were subjected to the SwissADME predictor. The analyses of the titled compounds were compared with that of the sulphathiazole, ciprofloxacin and fluconazole. The mean predicted lipophilicity values were assessed to decide the non-aqueous solubility of the compounds and were calculated by considering the consensus log P<sub>0</sub>/w. According to this, if molecule is more soluble, then its consensus log P<sub>0</sub>/w value will be more negative. The

results showed that the compounds are less soluble in non-aqueous solution and the order is MnL<sub>2</sub>>MnL<sub>1</sub>>L<sub>2</sub>>L<sub>1</sub>>ciprofloxacin>Fluconazole>STZ. To estimate the aqueous solubility log S scale was used: According to the log S scale, STZ, ciprofloxacin and fluconazole are soluble; the ligands are moderately soluble whereas the complexes are poorly soluble. (If log S < -10-poorly soluble, < -6, moderately soluble, < -4-soluble, < -2- very soluble, and < -0 highly soluble). Moreover, the topological polar surface areas (TPSAs) of the compounds were predicted to be in the range of 72.88-227.60 Å<sup>2</sup>. From these data we can deduce that the reference drugs have a very good intestinal absorption than the synthesized compounds. The ADMET lab predicted descriptors for the physicochemical properties as well as the optimal solubility of the ligand and its transition metal complexes were found to agree very well with the corresponding experimental results [35]. These results are presented in table 6.

**Table 6: Physicochemical Parameters Generated Using SwissADME Tool**

| Property         | STZ          | L1          | L2           | [Mn (L <sup>1</sup> ) <sub>2</sub> ].2H <sub>2</sub> O | [Mn (L <sup>2</sup> ) <sub>2</sub> ].2H <sub>2</sub> O | ciprofloxacin | Fluconazole  |
|------------------|--------------|-------------|--------------|--|--|---------------|--------------|
| Molecular weight | 255.33 g/mol | 361.42g/mol | 432.56 g/mol | 791.86 g/mol   | 882.99 g/mol   | 333.36 g/mol  | 306.27 g/mol |

|  |                       |                       |                       |                       |        |                      |                      |
|--|-----------------------|-----------------------|-----------------------|-----------------------|--------|----------------------|----------------------|
| Hydrogen bond donors                           | 2                     | 2                     | 2                     | 2                     | 1      | 2                    | 1                    |
| Hydrogen bond acceptors                        | 3                     | 5                     | 5                     | 10                    | 10     | 5                    | 7                    |
| Rotatable bonds                                | 3                     | 5                     | 8                     | 14                    | 19     | 3                    | 5                    |
| Log P (Partition coefficient, Predicted value) | 0.82                  | 2.36                  | 2.93                  | 3.48                  | 4.82   | 0.93                 | 0.88                 |
| Log S  | -3.43                 | -5.38                 | -6.20                 | -11.15                |        |                      | -3.54                |
| Molar refractivity                             | 68.84                 | 94.95                 | 123.98                | 205.86                | 239.58 | 97.06                | 70.71                |
| Topological polar surface area                 | 118.23 Å <sup>2</sup> | 124.80 Å <sup>2</sup> | 128.04 Å <sup>2</sup> | 227.60 Å <sup>2</sup> | 196.75 | 72.88 Å <sup>2</sup> | 81.65 Å <sup>2</sup> |

### 3.7.2: Pharmacokinetics evaluated using SwissADME, ADMETLAB 2.0 and vNN-ADMET

The pharmacokinetics parameters like absorption, skin permeation, distribution, and metabolism were predicted (Table 7). STZ, L1, ciprofloxacin, and fluconazole have high gastrointestinal (GI) absorption whereas L2, MnL1, and MnL2 have low gastrointestinal (GI) absorption. All the compounds are not BBB permeants, therefore, there is no possibility of causing harmful toxicants in the brain and bloodstream when metabolized. The skin permeability (log K<sub>p</sub>) values of the compound were found to be between -6.55 to -8.29 cm<sup>-1</sup>, deducing low skin permeability [36]. The permeability glycoprotein (P-gp) is an important protein that plays a significant role in drug absorption

and disposition. Hence, the compound was evaluated to determine whether the compound can act as a substrate or an inhibitor of P-gp, and the result revealed that the compounds are non-substrates of P-gp except MnL2, ciprofloxacin, and fluconazole. Interaction of molecules with cytochrome P450 (CYP) enzymes is essential because these isoenzymes may result in unwanted adverse side effects by lowering the solubility and the accumulation of the drug or its metabolites. Predictions revealed that STZ exhibits non-inhibitor for all the enzymes, L1 inhibits only CYP1A2, CYP2C9, and CYP3A4, L2 inhibits CYP2C19, CYP2C9, CYP2D6, and CYP2D6, MnL1 inhibits only CYP2C9, ciprofloxacin act as non-inhibitor whereas fluconazole inhibits CYP2C19 [37].

Table 7: Pharmacokinetics evaluated using SwissADME, ADMETLAB 2.0 and vNN-ADMET

| Property          | STZ  | L <sup>1</sup> | L <sup>2</sup> | [Mn (L <sup>1</sup> ) <sub>2</sub> ].2H <sub>2</sub> O | [Mn (L <sup>2</sup> ) <sub>2</sub> ].2H <sub>2</sub> O | ciprofloxacin | Fluconazole |
|-------------------|------|----------------|----------------|--|--|---------------|-------------|
| GI Absorption     | High | High           | Low            | Low  | Low  | High          | High        |
| BBB Permeant      | No   | No             | No             | No   | No   | No            | No          |
| P-gp Substrate    | No   | No             | No             | No   | Yes  | Yes           | Yes         |
| CYP1A2 inhibitor  | No   | Yes            | No             | No   | No   | No            | No          |
| CYP2C19 inhibitor | No   | No             | Yes            | No   | No   | No            | Yes         |
| CYP2C9 inhibitor  | No   | Yes            | Yes            | Yes  | Yes  | No            | No          |
| CYP2D6 inhibitor  | No   | No             | Yes            | No   | No   | No            | No          |
| CYP3A4 inhibitor  | No   | Yes            | Yes            | No   | No   | No            | No          |

|                                    |            |            |            |            |            |            |            |
|------------------------------------|------------|------------|------------|------------|------------|------------|------------|
| <b>Log KP</b><br>(Skin Permeation) | -7.82 cm/s | -6.91 cm/s | -6.74 cm/s | -7.05 cm/s | -6.55 cm/s | -8.53 cm/s | -7.92 cm/s |
|------------------------------------|------------|------------|------------|------------|------------|------------|------------|

**3.7.3 Drug-Likeness Evaluated SwissADME, ADMETLAB 2.0 and vNN-ADMET**

Druglikeness is a prediction that determines whether a particular pharmacological agent has properties consistent with being an orally active drug or not, in which this prediction is based on the Lipinski rule of five, Ghose filter, Veber’s rule, Egan, Muegge and

Bioavailability score. The SwissADME calculated results showed that the STZ, synthesized free ligand and the reference drugs satisfy Lipinski’s rule of five Ghose filter, Veber’s rule, Egan and Muegge with zero violations (Table 7), inferring that the synthesized compounds have a drug-like molecular nature. All the synthesized complexes violate some of these rules.

**Table 8: Drug-Likeness Evaluated SwissADME, ADMETLAB 2.0 and vNN-ADMET**

| Property                       | STZ          | L1           | L2           | [Mn (L <sup>1</sup> ) <sub>2</sub> ].2H <sub>2</sub> O | [Mn (L <sup>2</sup> ) <sub>2</sub> ].2H <sub>2</sub> O | Ciprofloxacin | Fluconazole  |
|--------------------------------|--------------|--------------|--------------|--|--|---------------|--------------|
| <b>Lipinski’s rule of five</b> | No violation | No violation | No violation | 2 violations: MW>500, NorO>10                          | 2 violations: MW>500, NorO>10                          | No violation  | No violation |
| <b>Ghose filter</b>            | No violation | No violation | No violation | 4 violations: MW>480, WLOGP>5.6, MR>130, #atoms>70     | 4 violations: MW>480, WLOGP>5.6, MR>130, #atoms>70     | No violation  | No violation |
| <b>Veber’s rule</b>            | No violation | No violation | No violation | 2 violations: Rotors>10, TPSA>140                      | 2 violations: Rotors>10, TPSA>140                      | No violation  | No violation |
| <b>Egan</b>                    | No violation | No violation | No violation | 2 violations: WLOGP>5.88, TPSA>131.6                   | 2 violations: WLOGP>5.88, TPSA>131.6                   | No violation  | No violation |
| <b>Muegge</b>                  | No violation | No violation | No violation | 3 violations: MW>600, XLOGP3>5, TPSA>150               | 4 violations: MW>600, XLOGP3>5, TPSA>150, Rotors>15    | No violation  | No Violation |
| <b>Bioavailability score</b>   | 0.55         | 0.55         | 0.55         | 0.17   | 0.17   | 0.55          | 0.55         |

**3.7.4: Toxicology Evaluated by SwissADME, ADMETLAB 2.0 and vNN-ADMET**

Toxicity prediction by computational technique is one of the new techniques in the drug development process, the modern era which consumes less time and low cost. Toxicity prediction of chemical entities is important to predict the amount of tolerability of the chemical entities before entering into in-vivo studies. The liver plays a critical role in energy exchanges and

the biotransformation of xenobiotics and drugs. Liver suffering from damage always disrupts normal metabolism and could even lead to liver failure. DILI and hepatotoxicity descriptors predicted that a molecule could present hepatotoxicity. Only L<sup>2</sup> and MnL<sup>2</sup> can have AMES Toxicity. All other results of the toxicity predictions (Table 9) showed that these compounds are less toxic [37].

**Table 9: Toxicology Evaluated by SwissADME, ADMETLAB 2.0 and vNN-ADMET**

| Property                | STZ | L <sup>1</sup> | L <sup>2</sup> | [Mn (L <sup>1</sup> ) <sub>2</sub> ].2H <sub>2</sub> O | [Mn (L <sup>2</sup> ) <sub>2</sub> ].2H <sub>2</sub> O | ciprofloxacin | Fluconazole |
|-------------------------|-----|----------------|----------------|--|--|---------------|-------------|
| <b>DILI</b>             | Yes | Yes            | Yes            | Yes  | Yes  | Yes           | Yes         |
| <b>AMES Toxicity</b>    | No  | No             | Yes            | No   | Yes  | No            | Yes         |
| <b>HERG 1 Inhibitor</b> | No  | No             | No             | No   | No   | No            | No          |

|  |                |              |              |             |             |              |                |
|--|----------------|--------------|--------------|-------------|-------------|--------------|----------------|
| <b>HERG 2 Inhibitor</b>                | No             | No           | No           | No          | No          | No           | No             |
| <b>Oral Rate Acute Toxicity (LD50)</b> | 1.905 mol/kg g | 2.368 mol/kg | 2.676 mol/kg | 2.86 mol/kg | 3.02 mol/kg | 2.128 mol/kg | 1.781 mol/kg g |
| <b>Hepatotoxicity</b>                  | Yes            | Yes          | Yes          | Yes         | Yes         | Yes          | Yes            |
| <b>Skin Sensitivity</b>                | No             | No           | No           | No          | No          | No           | No             |
| <b>T. Pyriformis Toxicity</b>          | -0.209         | 1.142        | 1.541        | 0.943       | 1.368       | 1.538        | 0.507          |

#### IV. CONCLUSION

The newly synthesized Schiff base ligands and their tridentate Mn (II) complexes were synthesized and structurally confirmed by the analytical and spectroscopic characterization techniques. The antimicrobial activities of the prepared compounds were screened against bacterial and fungal strains. The antimicrobial activity of the tested compounds revealed that the compounds are potent in inhibiting the growth of the microbes. The compound were predicted to display low toxicity levels and showed druglikeness according to the Lipinski Ghooose, Veber, Egan and Mugge rules with some violations only from the complexes. Thus, these in silico properties are appreciable.

#### Funding:

This research received no external funding.

#### Conflicts of Interest:

The authors declare no conflict of interest.

#### REFERENCES

- [1] El-Sonbati, A., Mahmoud, W., Mohamed, G. G., Diab, M., Morgan, S., & Abbas, S. (2019). Synthesis, characterization of Schiff base metal complexes and their biological investigation. *Applied Organometallic Chemistry*, e5048. <https://doi.org/10.1002/aoc.5048>
- [2] Al Zoubi, W., Al-Hamdani, A. A., Ahmed, S. D., & Ko, Y. G. (2017). Synthesis, characterization, and biological activity of Schiff bases metal complexes. *Journal of Physical Organic Chemistry*, 31(2), e3752. <https://doi.org/10.1002/poc.3752>
- [3] Zhang, H., Jeyakkumar, P., Vijaya Kumar, K., & Zhou, C. (2015). Synthesis of novel sulfonamide azoles via C–N cleavage of sulfonamides by azole ring and relational antimicrobial study. *New Journal of Chemistry*, 39(7), 5776-5796. <https://doi.org/10.1039/c4nj01932f>.
- [4] Rayati, S., & Ashouri, F. (2012). Pronounced catalytic activity of oxo-vanadium(IV) Schiff base complexes in the oxidation of cyclooctene and styrene by tert-butyl hydroperoxide. *Comptes Rendus Chimie*, 15(8), 679-687. <https://doi.org/10.1016/j.crci.2012.05.021>
- [5] Liu, Y., Wang, L., & Yin, D. (2022). Catalyst- and solvent-free synthesis, characterization, biological

activity of Schiff bases and their metal (II) complexes derived from ferrocene. <https://doi.org/10.21203/rs.3.rs-2317280/v1>

[6] Singh, U. P., & Malik, A. (2022). Pd(I) Schiff base complex anchored on mcm-41, a reusable catalyst for the heck reaction. *SSRN Electronic Journal*. <https://doi.org/10.2139/ssrn.4274111>

[7] Singh, P., & Quraishi, M. (2016). Corrosion inhibition of mild steel using novel bis Schiff's bases as corrosion inhibitors: Electrochemical and surface measurement. *Measurement*, 86, 114-124. <https://doi.org/10.1016/j.measurement.2016.02.052>

[8] Haruna, A., Rumah, M.M., Sani, U., & Ibrahim, A.K. (2021). Synthesis, characterization and corrosion inhibition studies on Mn (II) and Co (II) complexes derived from 1-[(Z)-[(2-hydroxyphenyl)imino]methyl]naphthalen-2-ol in 1M HCl solution. *International Journal of Biological, Physical and Chemical Studies*, 3(1), 09-18. <https://doi.org/10.32996/ijbpc.2021.3.1.2>

[9] Özkınalı, S., Yavuz, Ş., Tosun, T., Ali Köse, D., Gür, M., & Kocaokutgen, H. (2020). Synthesis, spectroscopic and thermal analysis and investigation of dyeing properties of o-hydroxy Schiff bases and their metal complexes. *ChemistrySelect*, 5(40), 12624-12634. <https://doi.org/10.1002/slct.202002470>

[10] Anacona, J., Mago, K., & Camus, J. (2018). Antibacterial activity of transition metal complexes with a tridentate NNO amoxicillin derived Schiff base. Synthesis and characterization. *Applied Organometallic Chemistry*, 32(7), e4374. <https://doi.org/10.1002/aoc.4374>

[11] Qian, H., & Sun, N. (2019). Synthesis and crystal structures of manganese(III) complexes derived from bis-schiff bases with antibacterial activity. *Transition Metal Chemistry*, 44(6), 501-506. <https://doi.org/10.1007/s11243-018-00296-x>

[12] Luo, X., Liu, Q., Han, Y., & Xue, L. (2020). Vanadium complexes derived from fluoro-substituted Schiff bases: Synthesis, crystal structures, and antimicrobial activity. *Inorganic and Nano-Metal Chemistry*, 50(9), 836-841. <https://doi.org/10.1080/24701556.2020.1726387>

[13] Mahjoub, S., Ansari, S., & Heshmatpour, F. (2016). Preparation, characterization, antibacterial and antifungal activities of some transition metal complexes with novel Schiff base ligand derived from N-amino rhodanine. *JOURNAL OF ADVANCES IN*

- CHEMISTRY, 11(7), 3723-3728. <https://doi.org/10.24297/jac.v11i7.2195>
- [14] Castro, J., Diz, M., Durán-Carril, M. L., Alvo, S., Bada, L., Viña, D., & García-Vázquez, J. A. (2022). Antitumor activity of Cu(II) complexes with Schiff bases derived from N'-tosylbenzene-1,2-Diamine. *SSRN Electronic Journal*. <https://doi.org/10.2139/ssrn.4163386>
- [15] Özbek, N., Alyar, S., Alyar, H., Şahin, E., & Karacan, N. (2013). Synthesis, characterization and antimicrobial evaluation of Cu(II), Ni(II), Pt(II) and Pd(II) sulfonylhydrazone complexes; 2D-QSAR analysis of Ni(II) complexes of sulfonylhydrazone derivatives. *Spectrochimica Acta Part A: Molecular and Biomolecular Spectroscopy*, 108, 123-132. <https://doi.org/10.1016/j.saa.2013.01.005>
- [16] Devi, J., Yadav, M., Kumar, D., Naik, L., & Jindal, D. (2018). Some divalent metal(II) complexes of salicylaldehyde-derived Schiff bases: Synthesis, spectroscopic characterization, antimicrobial and *in vitro* anticancer studies. *Applied Organometallic Chemistry*, 33(2), e4693. <https://doi.org/10.1002/aoc.4693>
- [17] Induleka R, I. R., Chandrika P, A. C., Tamilselvi M, T. M., Ushanandhini S, U. S., & Gowri M, G. M. (2022). Evaluation of Anticancer activity of Schiff bases derived from pyridine and their metal complexes- A review. *Oriental Journal Of Chemistry*, 38(3), 517-536. <https://doi.org/10.13005/ojc/380302>
- [18] Kunai, S., Nalamada, K., Reddy, R. S., Vindhya, H., & Raju, M. (2022). A schiff base derivation from 1,2-diaminobenzene and cephaclor as well as its transition metal complexes, were synthesis, magnetic studies and spectroscopic studies. *International Journal of Research in Pharmacy and Chemistry*, 12(3), 38-38. [https://doi.org/10.33289/ijrpc.12.3.2022.12\(38\)](https://doi.org/10.33289/ijrpc.12.3.2022.12(38))
- [19] Shukla, S., & Mishra, A. (2019). Metal complexes used as anti-inflammatory agents: Synthesis, characterization and anti-inflammatory action of vo(ii)-complexes. *Arabian Journal of Chemistry*, 12(7), 1715-1721. <https://doi.org/10.1016/j.arabjc.2014.08.020>
- [20] Amin Mir, M. (2022). Synthesis, catalysis and antimicrobial activity of 5d- metal chelate complex of Schiff base ligands. *Inorganic Chemistry Communications*, 142, 109594. <https://doi.org/10.1016/j.inoche.2022.109594>
- [21] Reiss, A., Cioateră, N., Dobrițescu, A., Rotaru, M., Carabet, A. C., Parisi, F., Gănescu, A., Dăbuleanu, I., Spînu, C. I., & Rotaru, P. (2021). Bioactive Co(II), Ni(II), and Cu(II) complexes containing a tridentate sulfathiazole-based (ONN) Schiff base. *Molecules*, 26(10), 3062. <https://doi.org/10.3390/molecules26103062>
- [22] Krátký, M., Dzurková, M., Janoušek, J., Konečná, K., Trejtnar, F., Stolaříková, J., & Vinšová, J. (2017). Sulfadiazine salicylaldehyde-based Schiff bases: Synthesis, antimicrobial activity and cytotoxicity. *Molecules*, 22(9), 1573. <https://doi.org/10.3390/molecules22091573>
- [23] Chohan, Z. H., Shad, H. A., & Supuran, C. T. (2011). Synthesis, characterization and biological studies of sulfonamide Schiff's bases and some of their metal derivatives. *Journal of Enzyme Inhibition and Medicinal Chemistry*, 27(1), 58-68. <https://doi.org/10.3109/14756366.2011.574623>
- [24] Digafie, Z., Melaku, Y., Belay, Z., & Eswaramoorthy, R. (2021). Synthesis, molecular docking analysis, and evaluation of antibacterial and antioxidant properties of stilbenes and Pinacol of quinolines. *Advances in Pharmacological and Pharmaceutical Sciences*, 2021, 1-17. <https://doi.org/10.1155/2021/6635270>
- [25] Tamene, D., & Endale, M. (2019). Antibacterial activity of coumarins and carbazole alkaloid from roots of *Clausena anisata*. *Advances in Pharmacological Sciences*, 2019, 1-8. <https://doi.org/10.1155/2019/5419854>
- [26] Zeleke, D., Eswaramoorthy, R., Belay, Z., & Melaku, Y. (2020). Synthesis and antibacterial, antioxidant, and molecular docking analysis of some novel quinoline derivatives. *Journal of Chemistry*, 2020, 1-16. <https://doi.org/10.1155/2020/1324096>
- [27] Tadavi, S. K., Bendre, R. S., Patil, S. V., Gaguna, S., & Rajput, J. D. (2020). Synthesis, crystal structures and antimicrobial activity of palladium metal complexes of sulfonyl hydrazone ligands. *European Journal of Chemistry*, 11(4), 377-384. <https://doi.org/10.5155/eurjchem.11.4.377-384.2040>
- [28] Kuchárová, V., Kuchár, J., Zaric, M., Canovic, P., Arsenijevic, N., Volarevic, V., Misirkic, M., Trajkovic, V., Radojević, I. D., Čomić, L. R., Matik, M., & Potočňák, I. (2019). Low-dimensional compounds containing bioactive ligands. Part XI: Synthesis, structures, spectra, *in vitro* anti-tumor and antimicrobial activities of 3d metal complexes with 8-hydroxyquinoline-5-sulfonic acid. *Inorganica Chimica Acta*, 497, 119062. <https://doi.org/10.1016/j.ica.2019.119062>
- [29] Bouone, Y. O., Bouzina, A., & Aouf, N. (2022). Synthesis, molecular docking analysis, ADMET and drug likeness prediction of a Benzenesulfonamide derivative analogue of SLC-0111. *ECMC 2022*. <https://doi.org/10.3390/ecmc2022-13407>
- [30] Loginova, N., Gvozdev, M., Osipovich, N., Khodosovskaya, A., Koval'chuk-Rabchinskaya, T., Ksendzova, G., Kotsikau, D., & Evtushenkov, A. (2022). Silver(I) complexes with phenolic Schiff bases: Synthesis, anti-bacterial evaluation and interaction with biomolecule s. *ADMET and DMPK*. <https://doi.org/10.5599/admet.1167>
- [31] Ommenya, F. K., Nyawade, E. A., Andala, D. M., & Kinyua, J. (2020). Synthesis, characterization and antibacterial activity of Schiff base, 4-Chloro-2-[(E)-(4-Fluorophenyl)imino]methyl}phenol metal (II)

complexes. *Journal of Chemistry*, 2020, 1-8. <https://doi.org/10.1155/2020/1745236>

[32] Mahmoud, W. H., Deghadi, R. G., & Mohamed, G. G. (2018). Metal complexes of novel Schiff base derived from iron sandwiched organometallic and 4-nitro-1,2-phenylenediamine: Synthesis, characterization, DFT studies, antimicrobial activities and molecular docking. *Applied Organometallic Chemistry*, 32(4), e4289. <https://doi.org/10.1002/aoc.4289>

[33] Nazeer M. (2021). IR, UV and CV studies of Schiff base metal complexes derived from o-phenylenediamine with chlorobenzaldehyde. *JOURNAL OF ADVANCED APPLIED SCIENTIFIC RESEARCH*, 1(9). <https://doi.org/10.46947/joaasr19201774>

[34] Abdel-Monem, R. A., Khalil, A. M., Darwesh, O. M., Hashim, A. I., & Rabie, S. T. (2019). Antibacterial properties of carboxymethyl chitosan schiff-base nanocomposites loaded with silver

nanoparticles. *Journal of Macromolecular Science, Part A*, 57(2), 145-155. <https://doi.org/10.1080/10601325.2019.1674666>

[35] Daina, A., Michielin, O., & Zoete, V. (2017). SwissADME: A free web tool to evaluate pharmacokinetics, drug-likeness and medicinal chemistry friendliness of small molecules. *Scientific Reports*, 7(1). <https://doi.org/10.1038/srep42717>

[36] Eswaramoorthy, R., Hailekiros, H., Kedir, F., & Endale, M. (2021). In silico molecular docking, DFT analysis and ADMET studies of carbazole alkaloid and coumarins from roots of *Clausena anisata*: A potent inhibitor for quorum sensing. *Advances and Applications in Bioinformatics and Chemistry*, 14, 13-24. <https://doi.org/10.2147/aabc.s290912>

[37] Fekadu, M., Zeleke, D., Abdi, B., Guttula, A., Eswaramoorthy, R., & Melaku, Y. (2022). undefined. *BMC*

*Chemistry*, 16(1). <https://doi.org/10.1186/s13065-022-00795-0>